

= *i*-Pr, 97782-75-7; 2 (R = cyclohexyl, R' = (CH₂)₃OAc), 97782-76-8; 2 (R = Ph, R' = *i*-Pr), 97782-77-9; 2 (R = Ph, R' = (CH₂)₃OH), 97782-78-0; 2 (R = R' = *i*-Pr), 97782-79-1; 2 (R = *t*-Bu, R' = (CH₂)₃OH), 97782-74-6; 2 (R = Ph, R' = (CH₂)₃OH), 97782-80-4; MeB(OMe)₂, 7318-81-2; MeB(OEt)₂, 86595-26-8; MeB(OPr-*i*)₂, 86595-27-9; MeB(OBu-*t*)₂, 819-38-5; MeLi, 917-54-4; *n*-BuB(OPr-*i*)₂, 86595-32-6; *t*-BuB(OPr-*i*)₂, 86595-34-8; PhB(OPr-*i*)₂, 1692-26-8; *i*-PrLi, 1888-75-1; *t*-BuLi, 594-19-4; PhLi, 591-51-5; 2-methyl-1,3,2-dioxaborolane, 37003-57-9; 2-methyl-1,3,2-dioxaborinane, 51901-48-5; 2-methyl-1,3,2-dioxatetramethylborolane, 94242-85-0; 2-methyl-1,3,2-benzodioxaborole, 51901-49-6; 2-*n*-butyl-1,3,2-dioxaborinane, 30169-71-2; *tert*-butyl-1,3,2-dioxaborinane, 63689-73-6; cyclohexyldiisopropoxyborane, 97782-70-2; 2-cyclohexyl-1,3,2-dioxaborinane, 30169-75-6; 2-phenyl-1,3,2-dioxaborinane, 4406-77-3; *n*-butylisopropoxyborane, 97782-81-5; *n*-butyl-*tert*-butylisopropoxyborane, 97782-82-6; *n*-butylphenylisopropoxyborane, 97782-83-7; *n*-bu-

tyl-*tert*-butyl(3-hydroxypropoxy)borane, 97782-84-8; *n*-butylphenyl(3-hydroxypropoxy)borane, 97782-85-9; *n*-butylisopropyl(3-hydroxypropoxy)borane, 97782-86-0; *tert*-butylisopropylisopropoxyborane, 97782-87-1; di-*tert*-butylisopropoxyborane, 86595-35-9; *tert*-butylphenylisopropoxyborane, 97782-88-2; di-*tert*-butyl(3-hydroxypropoxy)borane, 97782-89-3; *tert*-butylphenyl(3-hydroxypropoxy)borane, 97782-90-6; *tert*-butylisopropyl(3-hydroxypropoxy)borane, 97782-91-7; cyclohexylisopropylisopropoxyborane, 97782-92-8; *tert*-butylcyclohexylisopropoxyborane, 97782-93-9; phenylcyclohexylisopropoxyborane, 97782-94-0; *tert*-butylcyclohexyl(3-hydroxypropoxy)borane, 97782-95-1; isopropylcyclohexyl(3-hydroxypropoxy)borane, 97782-99-5; phenylcyclohexyl(3-hydroxypropoxy)borane, 97782-96-2; phenylisopropylisopropoxyborane, 97782-97-3; diphenylisopropoxyborane, 69737-51-5; isopropylphenyl(3-hydroxypropoxy)borane, 97782-98-4; diphenyl(3-hydroxypropoxy)borane, 74666-84-5; acetyl chloride, 75-36-5; benzoyl chloride, 98-88-4.

(μ -H)₂M₃(CO)₈(μ -PPh₂)₂ (M = Fe, Ru, Os): An Isostructural Triad of Phosphido-Bridged Hydrides. Rational Synthesis and Structural Characterization

Vikram D. Patel, Andrew A. Cherkas, Donato Nucciarone, Nicholas J. Taylor, and Arthur J. Carty*

Guelph-Waterloo Centre for Graduate Work in Chemistry, Waterloo Campus, Department of Chemistry, University of Waterloo, Waterloo, Ontario, Canada N2L 3G1

Received January 21, 1985

The synthesis and structural characterization of the triad of phosphido-bridged hydrido clusters (μ -H)₂M₃(CO)₈(μ -PPh₂)₂ (1, M = Fe, 2, M = Ru, and 3, M = Os) are described. The triiron cluster 1 has been prepared via the reaction of Ph₂PH with the protonated anion Fe₄(CO)₁₃²⁻. The ruthenium and osmium congeners have been obtained from the phosphine complexes M₃(CO)₁₀(PPh₂H)₂ via oxidative addition of the P-H bonds of the secondary phosphines to the clusters. Crystals of 1-3 are triclinic of space group P $\bar{1}$ with unit cell dimensions. 1: *a* = 10.918 (2) Å, *b* = 11.898 (2) Å, *c* = 14.705 (2) Å; α = 75.02 (1)°, β = 84.72 (1)°, γ = 70.84 (1)°. 2: *a* = 11.150 (1) Å, *b* = 12.027 (1) Å, *c* = 14.693 (1) Å; α = 76.03 (1)°, β = 84.70 (1)°, γ = 70.24 (1)°. 3: *a* = 11.184 (1) Å, *b* = 11.991 (1) Å, *c* = 14.657 (1) Å; α = 76.17 (1)°, β = 84.72 (1)°, γ = 70.01 (1)°. The structures were solved and refined to the following *R* and *R*_w values; 1, *R* = 0.034, *R*_w = 0.039 on 4243 observed (*I* ≥ 3σ(*I*)) data; 2, *R* = 0.023, *R*_w = 0.027 on 5478 data; 3, *R* = 0.038, *R*_w = 0.048 on 5325 data. The three molecules are isostructural with a triangular framework of metal atoms supported on two adjacent sides by phosphido and hydrido bridges, one metal-metal vector being unbridged. The change in structural parameters down the triad and reactions with carbon monoxide are discussed.

Introduction

The search for strongly bound yet flexible bridging ligands capable of maintaining two or more metal fragments in close proximity both within and beyond the regimes of metal-metal bonding has stimulated interest in the chemistry of phosphido-bridged systems.¹ Although there is now abundant evidence that phosphido bridges may be noninnocent ligands^{1,2} and hence cannot be discounted as

sites of reactivity, there are also substantial indications of potentially useful chemical transformations on PR₂-bridged bi- and polynuclear compounds.^{1,3}

One class of phosphido-bridged compounds which has not yet attracted much attention is the group of μ -hydrido,

(1) See, for example: (a) Geoffroy, G. L.; Rosenberg, S.; Shulman, P. M.; Whittle, R. R. *J. Am. Chem. Soc.* **1984**, *106*, 1519. (b) Yu, Y. F.; Galluci, J.; Wojcicki, A. *J. Chem. Soc., Chem. Commun.* **1984**, 653. (c) Henrick, K.; Iggo, K.; Mays, M. J.; Raithby, P. R. *J. Chem. Soc., Chem. Commun.* **1984**, 209. (d) Bender, R.; Braunstein, P.; Metz, B.; Lemoine, P. *Organometallics* **1984**, *3*, 381. (e) Muller, M.; Vahrenkamp, H. *Chem. Ber.* **1983**, *116*, 2311. (f) Kreter, P. E.; Meek, D. W. *Inorg. Chem.* **1983**, *22*, 319. (g) Haines, R. J.; Steen, N. D. C. T.; English, R. B. *J. Chem. Soc., Chem. Commun.* **1981**, 587. (h) Jones, R. A.; Wright, T. C.; Atwood, J. L.; Hunter, W. E. *Organometallics* **1983**, *2*, 470. (i) Carty, A. J. *Adv. Chem. Ser.* **1982**, No. 196, 163. (j) Carty, A. J. *Pure Appl. Chem.* **1982**, *54*, 113. (k) Elinget, B.; Werner, H. *J. Organomet. Chem.* **1983**, *252*, C47.

(2) (a) Smith, W. F.; Taylor, N. J.; Carty, A. J. *J. Chem. Soc., Chem. Commun.* **1976**, 896. (b) Yasufuku, K.; Yamazaki, H. *J. Organomet. Chem.* **1972**, *35*, 367. (c) Yu, Y. F.; Galluci, J.; Wojcicki, A. *J. Am. Chem. Soc.* **1983**, *105*, 4826. (d) Harley, A. D.; Guskey, G. J.; Geoffroy, G. L. *Organometallics* **1983**, *2*, 53. (e) McKennis, J. S.; Kyba, E. V. *Organometallics* **1983**, *2*, 1249. (f) Regragui, R.; Dixneuf, P. H.; Taylor, N. J.; Carty, A. J. *Organometallics* **1984**, *3*, 814. (g) MacLaughlin, S. A.; Carty, A. J.; Taylor, N. J. *Can. J. Chem.* **1982**, *60*, 87.

(3) (a) Mott, G. N.; Granby, R.; MacLaughlin, S. A.; Taylor, N. J.; Carty, A. J. *Organometallics* **1983**, *2*, 189. (b) Nucciarone, D.; Taylor, N. J.; Carty, A. J. *Organometallics* **1984**, *3*, 177. (c) Collman, J. P.; Rothrick, R. K.; Finke, R. G.; Rose-Munch, F. J. *J. Am. Chem. Soc.* **1977**, *99*, 7381. (d) Collman, J. P.; Rothrock, R. K.; Finke, R. G.; Moore, E. J.; Rose-Munch, F. *Inorg. Chem.* **1982**, *21*, 146. (e) MacLaughlin, S. A.; Johnson, J. P.; Taylor, N. J.; Carty, A. J.; Sappa, E. *Organometallics* **1983**, *2*, 352. (f) Roberts, D. A.; Steinmetz, G. R.; Breen, M. J.; Shulman, P. M.; Morrison, E. D.; Duttera, M. R.; DeBrosse, C. W.; Whittle, R. W.; Geoffroy, G. L. *Organometallics* **1983**, *2*, 846.

μ -phosphido clusters. On the basis of the known chemistry of metal hydrides, hydrido phosphides would almost certainly be involved in any stoichiometric or catalytic hydrogenation process involving a phosphido-bridged cluster. Relatively few hydrido, μ -phosphido clusters are known, and rational high yield routes to such compounds have rarely been described. For the iron triad elements most of the known compounds are ruthenium clusters. Phosphido-bridged dimers with terminal hydrides have been produced via the acidification of anions derived from $\text{Fe}_2(\text{CO})_6(\text{PRR}')_2$ reductions^{1b,2c,e} and H_2 addition to the heterometallic dimer $(\text{CO})_3(\text{PPh}_3)\text{Fe}(\mu\text{-PPh}_2)\text{Ir}(\text{CO})\text{Cl}(\text{Ph}_3\text{P})$,^{3f} and a trinuclear hydride, $\text{HF}_3(\text{CO})_7(\mu\text{-PPh}_2)_3$, of uncertain structure was obtained on treatment of $\text{Na}[\text{Fe}_2(\mu\text{-PPh}_2)_2(\text{CO})_5[\text{C}(\text{O})\text{R}]] \cdot 2\text{THF}$ with CF_3COOH .^{3d}

Vahrenkamp has reported the synthesis of $(\mu\text{-H})_2\text{Fe}_3(\text{CO})_8(\mu\text{-PMe}_2)_2$ in 1% yield from $\text{Fe}_3(\text{CO})_{12}$ and PMe_2H .⁴ The closely related ruthenium complex $(\mu\text{-H})_2\text{Ru}_3(\text{CO})_8(\mu\text{-PPh}_2)_2$, which could not be separated from $\text{Ru}_2(\text{CO})_6(\mu\text{-PPh}_2)_2$, was one of several products from the photolysis of $\text{Ru}_3(\text{CO})_9(\text{PPh}_2\text{H})_3$.^{5a} The same reaction afforded small amounts of $(\mu\text{-H})\text{Ru}_3(\text{CO})_7(\mu\text{-PPh}_2)_3$, which has a triangular Ru_3 skeleton bridged on all three sides by $\mu\text{-PPh}_2$ groups,^{5b} and $(\mu\text{-H})_2\text{Ru}_3(\text{CO})_7(\mu\text{-PPh}_2)_2(\text{PPh}_2\text{H})$, a phosphine substitution product of $(\mu\text{-H})_2\text{Ru}_3(\text{CO})_8(\mu\text{-PPh}_2)_2$.^{5a} After completion of the present work Haines and co-workers^{5b} reported briefly the isolation of $(\mu\text{-H})_2\text{Ru}_3(\text{CO})_8(\mu\text{-PPh}_2)_2$ and $(\mu\text{-H})\text{Ru}_3(\text{CO})_7(\mu\text{-PPh}_2)_3$ from the thermal reaction of $\text{Ru}_3(\text{CO})_{12}$ with PPh_2H . Bonnet⁶ has recently made the interesting observation that hydrogenation of $\text{Ru}_3(\text{CO})_8(\text{Ph}_2\text{PCH}_2\text{PPh}_2)_2$ at 85 °C affords good yields of the stable phosphido cluster $(\mu\text{-H})_2\text{Ru}_3(\text{CO})_6(\mu\text{-P}(\text{Ph})\text{CH}_2\text{PPh}_2)_2$ which contains two phosphido phosphine ligands and is a hydrogenation catalyst. The monohydrido species $(\mu\text{-H})\text{M}_3(\text{CO})_{10}(\mu\text{-PRH})$ ($\text{M} = \text{Ru}$, $\text{R} = \text{Ph}$; $\text{M} = \text{Os}$, $\text{R} = \text{Ph}$, $\text{CH}_3\text{OC}_6\text{H}_4$, C_6H_{11}) have been described in detail by Mays⁷ and Huttner⁸ as intermediates en route to the μ_3 -phosphinidene compounds $(\mu\text{-H})_2\text{M}_3(\text{CO})_9(\mu_3\text{-PR})$. The corresponding $(\mu\text{-H})\text{Ru}_3(\text{CO})_{10}(\mu\text{-PPh}_2)$ compound, on treatment with Me_3NO , loses one molecule of CO to give the remarkable unsaturated and highly reactive cluster $(\mu\text{-H})\text{Ru}_3(\text{CO})_9(\mu\text{-PPh}_2)$.⁹

As part of our program on phosphido-bridged cluster chemistry and with a possible extension of the novel behavior of $(\mu\text{-H})\text{Ru}_3(\text{CO})_9(\mu\text{-PPh}_2)$ to other systems in mind, we have undertaken to develop useful synthetic routes to a range of bis(phosphido)-bridged dihydrides. In this paper we describe the synthesis and X-ray characterization of the isostructural family of compounds $(\mu\text{-H})_2\text{M}_3(\text{CO})_8(\mu\text{-PPh}_2)_2$ ($\text{M} = \text{Fe}$, Ru , Os). This series of readily accessible and structurally analogous molecules should provide an opportunity, relatively rare in organometallic chemistry, for a comparison of reactivity changes within a transition-metal triad.

Experimental Section

General Procedure. All reactions were carried out under an atmosphere of dry nitrogen using Schlenk techniques. Benzene,

Table I. Spectroscopic Data for $(\mu\text{-H})_2\text{M}_3(\text{CO})_8(\mu\text{-PPh}_2)_2$ Complexes

compd	$\delta(^1\text{H})$	$\delta(^{31}\text{P}\{^1\text{H}\})$	IR $\nu(\text{CO})$, ^c cm^{-1}
1, $\text{M} = \text{Fe}$	-20.70 (t, 2 H) ^a (² $J_{\text{P-H}} = 41.80$ Hz) 7.2-8.2 (m, 20 H)	+203.20 ^a	2059 m, 2019 s, 1996 m, 1983 w, 1970 m
2, $\text{M} = \text{Ru}$	-16.15 (t, 2 H) ^a (² $J_{\text{P-H}} = 23.0$ Hz) 6.9-8.1 (m, 20 H)	+163.70 ^a	2076 s, 2043 s, 2027 s, 2014 s, 1987 m, 1973 m
3, $\text{M} = \text{Os}$	-17.30 (t, 2 H) ^b (² $J_{\text{P-H}} = 13.70$ Hz) 7.3-7.95 (m, 20 H)	+63.80 ^b	2078 s, 2043 vs, 2017 s, 2008 s, 1979 m, 1958 m

^aIn C_6D_6 . ^bIn CDCl_3 . ^cIn C_6H_{12} .

cyclohexane, decalin, and THF were dried and purified by distillation from sodium benzophenone ketyl under nitrogen. Heptane and toluene were dried by distillation from LiAlH_4 under nitrogen. Metal carbonyls ($\text{Fe}(\text{CO})_5$, $\text{Ru}_3(\text{CO})_{12}$, $\text{Os}_3(\text{CO})_{12}$) and diphenylphosphine were obtained from Strem Chemicals. The compounds $[(\text{Ph}_3\text{P})_2\text{N}]_2\text{Fe}_4(\text{CO})_{13}$ ¹⁰ and $\text{Os}_2(\text{CO})_{10}(\text{NCMe})_2$ ¹¹ were prepared by literature methods. Infrared spectra were recorded in solution on a Perkin-Elmer PE 180 spectrometer using 0.1-mm path length matched sodium chloride cells. NMR spectra were recorded on a Bruker WP-80 instrument operating at 80 MHz for ^1H and 32.38 MHz for ^{31}P . Proton chemical shifts are relative to external Me_4Si and ^{31}P shifts to 85% H_3PO_4 . Elemental analyses were performed by Guelph Chemical Laboratories.

Synthesis of $(\mu\text{-H})_2\text{Fe}_3(\text{CO})_8(\mu\text{-PPh}_2)_2$ (1). To a slurry of $[(\text{Ph}_3\text{P})_2\text{N}]_2[\text{Fe}_4(\text{CO})_{13}]$ (3.0 g, 1.8 mmol) in THF (150 mL), maintained at 0 °C (ice/water slush), was added Ph_2PH (0.93 mL, 5.4 mmol) followed by excess trifluoroacetic acid (4.0 mL, 52 mmol). This rapidly gave a dark brown solution, which turned dark green on warming to room temperature. After the solution was stirred for an additional 3 h at room temperature, the volatiles were removed under vacuum. The resultant oily dark green residue was extracted with warm heptane (2×75 mL) and, chromatographed over a 3×30 cm column of Florisil, with 1:1 heptane/toluene as eluant. The first yellow band removed contained $\text{Fe}(\text{CO})_4(\text{PPh}_2\text{H})$, which was identified by comparison with the reported infrared spectrum.¹² The band containing 1 eluted next. The solution was stripped to dryness under vacuum, and the resultant dark green solid was redissolved in heptane (20 mL) and refrigerated at -10 °C. Well-formed crystals of 1 separated, which were collected by filtration and dried under vacuum; yield 0.80 g (60%). Anal. Calcd for $\text{C}_{32}\text{H}_{22}\text{Fe}_3\text{P}_2\text{O}_8$: C, 50.30; H, 2.88; P, 8.10. Found: C, 50.10; H, 3.00; P, 8.30. Spectroscopic data for the compounds 1, 2, and 3 are listed in Table I.

Synthesis of $\text{Ru}_3(\text{CO})_{10}(\text{HPPH}_2)_2$. The ketyl route of Bruce et al.¹³ was used to prepare $\text{Ru}_3(\text{CO})_{10}(\text{PPh}_2\text{H})_2$. To a 100 mL, two-necked flame-dried, round-bottom flask equipped with magnetic stirring bar and under a positive pressure of nitrogen was added $\text{Ru}_3(\text{CO})_{12}$ (200 mg, 0.33 mmol) and THF (30 mL). Upon complete dissolution of $\text{Ru}_3(\text{CO})_{12}$, 2 equiv of PPh_2H (58 μL) was added. With rapid stirring, a catalytic amount of purple sodium benzophenone ketyl was added. Three to four drops usually sufficed to give the disubstituted cluster. The solution was allowed to stir for ~10 min then taken to dryness, and chromatographed on a Florisil column, eluting with heptane. Upon removal of $\text{Ru}_3(\text{CO})_{12}$ and $\text{Ru}_3(\text{CO})_{11}(\text{HPPH}_2)$ as minor products, the column was then eluted with a 1:1 benzene/toluene solution to remove $\text{Ru}_3(\text{CO})_{10}(\text{HPPH}_2)_2$; yield 0.114 g (38%); IR (C_6H_{12}) $\nu(\text{CO})$ 2074 (w), 2039 (w), 2020 (s), 1999 (s, br), 1973 (m, sh), 1961 (m, sh) cm^{-1} ; $^{31}\text{P}\{^1\text{H}\}$ NMR (C_6D_6 , 313 K) δ 5.1 (s). Anal. Calcd for $\text{C}_{34}\text{H}_{22}\text{Ru}_3\text{P}_2\text{O}_{10}$: C, 42.73; H, 2.32; P, 6.48. Found: C, 42.96; H, 2.46; P, 6.86.

Synthesis of $(\mu\text{-H})_2\text{Ru}_3(\text{CO})_8(\mu\text{-PPh}_2)_2$ (2). A solution of $\text{Ru}_3(\text{CO})_{10}(\text{PPh}_2\text{H})_2$ (0.4 g, 0.626 mmol) in toluene (50 mL) was

(10) Whitmire, K.; Ross, J.; Cooper, C. B., III; Shriver, D. F. *Inorg. Chem.* **1982**, *21*, 66.

(11) (a) Tachikawa, M.; Shapley, J. R. *J. Organomet. Chem.* **1977**, *124*, C19. (b) Aime, S.; Deeming, A. J. *J. Chem. Soc., Dalton Trans.* **1983**, 1807.

(12) Smith, J. G.; Thompson, D. T. *J. Chem. Soc. A* **1967**, 1694.

(13) Bruce, M. I.; Kehoe, D. C.; Matisons, J. G.; Nicholson, B. K.; Rieger, P. H.; Williams, M. L. *J. Chem. Soc., Chem. Commun.* **1982**, 442.

(4) Keller, E.; Vahrenkamp, H. *Chem. Ber.* **1981**, *114*, 1124.

(5) (a) Rosen, R. P.; Geoffroy, G. L.; Bueno, C.; Churchill, M. R.; Ortega, R. B. *J. Organomet. Chem.* **1983**, *254*, 89. (b) Field, J. S.; Haines, R. J.; Moore, M. H.; Smit, D. N.; Steer, L. M. *S. Afr. J. Chem.* **1984**, *37*, 138.

(6) Lavigne, G.; Lugan, N.; Bonnet, J. J. *Organometallics* **1982**, *1*, 1040.

(7) Iwasaki, F.; Mays, M. J.; Raithby, P. R.; Taylor, P. L.; Wheatley, P. J. *J. Organomet. Chem.* **1981**, *213*, 185.

(8) Natarajan, K.; Zolnai, L.; Huttner, G. *J. Organomet. Chem.* **1981**, *220*, 365.

(9) MacLaughlin, S. A.; Taylor, N. J.; Carty, A. J. *Organometallics* **1984**, *3*, 392.

Table II. Crystallographic Data for $(\mu\text{-H})_2\text{M}_3(\text{CO})_8(\mu\text{-PPh}_2)_2$ (1, M = Fe; 2, M = Ru; 3, M = Os)

	1	2	3
mol formula	$\text{Fe}_3\text{P}_2\text{O}_8\text{C}_{32}\text{H}_{22}0.5\text{C}_7\text{H}_8$	$\text{Ru}_3\text{P}_2\text{O}_8\text{C}_{32}\text{H}_{22}0.5\text{C}_7\text{H}_8$	$\text{Os}_3\text{P}_2\text{O}_8\text{C}_{32}\text{H}_{22}0.5\text{C}_7\text{H}_8$
mol wt	810.09	945.76	1213.15
crystal size, mm ³	0.18 × 0.28 × 0.30	0.22 × 0.25 × 0.28	sphere 0.21 ± 2 (epoxy coated)
space group	$P\bar{1}$	<i>a</i>	<i>a</i>
cell dimens			
<i>a</i> , Å	10.918 (2)	11.150 (1)	11.184 (1)
<i>b</i> , Å	11.898 (2)	12.027 (1)	11.991 (1)
<i>c</i> , Å	14.705 (3)	14.693 (1)	14.657 (1)
α , deg	75.02 (1)	76.03 (1)	76.17 (1)
β , deg	84.72 (1)	84.70 (1)	84.72 (1)
γ , deg	70.84 (1)	70.24 (1)	70.01 (1)
vol, Å ³	1743.0 (5)	1799.4 (3)	1793.7 (3)
<i>Z</i>	2	<i>a</i>	<i>a</i>
ρ_{measd} , g·cm ⁻³	1.52	1.74	2.24
ρ_{calcd} , g·cm ⁻³	1.53	1.745	2.246
monochromator	single-crystal graphite	<i>a</i>	<i>a</i>
2 θ range, deg	50	<i>a</i>	<i>a</i>
scan type	θ -2 θ	<i>a</i>	<i>a</i>
scan speed, deg min ⁻¹	variable 2.93-29.3	<i>a</i>	<i>a</i>
scan width, deg	[2 θ (Mo K α_1) - 0.8] to [2 θ (Mo K α_2) + 0.8]	<i>a</i>	<i>a</i>
stds	35 $\bar{2}$, 423	1 $\bar{2}$ 7, 37 $\bar{1}$	1 $\bar{6}$ 1, 433
change of intensity of stds	±2%	±2%	-9%
measd data	6151	6383	6374
obsd data (<i>I</i> ≥ 3 σ (<i>I</i>))	4243	5478	5325
μ (Mo K α), cm ⁻¹	14.07	13.53	114.12 ($\mu R = 1.2$)
<i>F</i> (000)	822	930	1122
residual density, e·Å ⁻³	0.4	0.5	2.6
<i>R</i>	0.034	0.023	0.038
<i>R</i> _w	0.039	0.027	0.048
<i>w</i> ⁻¹	1.8 - 0.028 <i>R</i> _o + 0.0007 <i>F</i> _o ²	1.88 - 0.021 <i>F</i> _o + 0.00037 <i>F</i> _o ²	1.9 - 0.021 <i>F</i> _o + 0.00021 <i>F</i> _o ²

^a Same as for 1.

stirred at 70 °C for 18 h under N₂. Toluene was subsequently removed and the slurry diluted with ca. 10 mL of heptane. This solution was chromatographed on a 3 × 20 cm column of Florisil, eluting with heptane. The first, yellow band contained a mixture of 2 and Ru₂(CO)₆(PPh₂)₂,¹⁴ which were separated by fractional crystallization from heptane/toluene when orange crystals of 2 precipitated preferentially. Small amounts of two minor products, subsequently eluted, have not yet been characterized; yield 0.12 g (30%). Anal. Calcd for C₃₂H₂₂Ru₃P₂O₈: C, 42.72; H, 2.46; P, 6.89. Found: C, 42.86; H, 2.42; P, 6.80.

Synthesis of Os₃(CO)₁₀(Ph₂PH)₂. Os₃(CO)₁₀(NCMe)₂ was prepared by the method described by Aime and Deeming.^{11b} Os₃(CO)₁₀(NCMe)₂ (0.671 g, 0.719 mmol) was mixed as a slurry in 50 mL of C₆H₆. Ph₂PH (250 μL) was added and the mixture stirred for 24 h at room temperature. The now yellow-orange solution was concentrated to 5 mL and chromatographed on a fresh Florisil column eluting first with heptane to remove a small amount of yellow Os₃(CO)₁₁(Ph₂PH) as the first band. Then a 70:30 benzene/heptane solution was used to elute the Os₃(CO)₁₀(Ph₂PH)₂. The solution was concentrated to 5 mL, 15 mL of heptane added, and the solution concentrated again and cooled at -10 °C until a solid precipitated out. The solid was washed with 2 × 1 mL of pentane and dried in vacuo: yield 0.378 g of Os₃(CO)₁₀(Ph₂PH)₂, 50% from Os₃(CO)₁₂; IR (C₆H₁₂) ν (CO) 2086 (w), 2067 (vw), 2024 (s), 2013 (m, sh), 2003 (vs), 1967 (s), 1953 (w, sh), 1943 (w, sh) cm⁻¹; ³¹P{¹H} NMR (C₆D₆, 313 K) δ -37.92 (s); ¹H NMR (CDCl₃, 313 K) δ 7.40 (d, *J*_{PH} = 383.8 Hz, PH), 7.7-7.2 (m, PhH). Anal. Calcd for C₃₄H₂₂O₁₀Os₃P₂: C, 33.39; H, 1.81; P, 5.06. Found: C, 33.80; H, 1.93; P, 5.16.

Synthesis of $(\mu\text{-H})_2\text{Os}_3(\text{CO})_8(\mu\text{-PPh}_2)_2$ (3). A slurry of Os₃(CO)₁₀(Ph₂PH)₂ (0.671 g, 0.24 mmol) in decalin (25 mL) under N₂ was heated from 25 to 160 °C over a period of 4 h. The orange solution was cooled to room temperature and the decalin removed under vacuum. The orange solid was dissolved in cyclohexane and chromatographed on a 3 cm × 15 cm column of Florisil eluting with cyclohexane. A yellow band of HOs₃(CO)₁₀(Ph₂P)_{7.8} was eluted first. A 1:1 benzene/heptane mixture brought down a second band of the required complex; yield 0.174 g (60%). Anal.

Calcd for C₃₂H₂₂Os₃P₂O₈: C, 32.94; H, 1.90; P, 5.31. Found: C, 32.85; H, 1.99; P, 5.39.

Reactions of $(\mu\text{-H})_2\text{M}_3(\text{CO})_8(\mu\text{-PPh}_2)_2$ (1, M = Fe; 2, M = Ru, 3, M = Os) with CO. Carbon monoxide (1 atm) was purged through solutions of 1 [(0.1 g; heptane), 2 (0.05 g; toluene), and 3 (0.05 g; toluene)] at 25 °C and the reactions monitored by infrared and ³¹P NMR spectroscopy. Under these conditions only 1 reacts, as evidenced by the appearance of additional bands in the IR [1966 (m), 1958 (w) cm⁻¹] and a singlet resonance at δ +279.4 in the ³¹P NMR spectrum (C₆D₆) characteristic of Fe₃(CO)₉(μ -PPh₂)₂ (4). Integration of ³¹P NMR resonances indicated a 30% conversion of 1 to 4 after 48 h. In an independent experiment, 1 was heated to 60 °C while CO was purged through the heptane solution. Under these conditions 1 is converted to 4 in essentially quantitative yield within 3 h, as indicated by a change of color from green 1 to orange 4 and by IR [ν (CO) 2057 (s), 2018 (s), 1997 (m), 1966 (m), 1958 (w) cm⁻¹] and ³¹P NMR spectroscopy. In the room-temperature spectra, the higher wavelength bands of 4 in the IR are masked by those of 1. For 2 and 3 no spectral changes were observed on further heating to 80 °C for 96 h.

X-ray Structural Analyses of 1, 2, and 3. Dark green crystals of 1 were grown from toluene/heptane solutions at -5 °C. A suitable crystal was attached to a glass fiber, mounted on a brass pin in a goniometer head, and centered on a Syntex P2₁ diffractometer. The Syntex auto indexing and cell refinement procedures identified and refined a triclinic unit cell from a set of 15 reflections well dispersed in reciprocal space. Subsequent checks of axial reflections confirmed the lack of systematic absences expected for the triclinic system. An orange crystal of 2 was obtained by crystallization from a toluene/heptane solution. For 3 crystals from toluene were pale yellow. Examination of diffraction data for 2 and 3 also revealed the presence of triclinic cells. The refined unit cells for 2 and 3 (Table II) suggest that all three crystals are isomorphous. The increase in unit cell volume from the iron cluster 1 to the osmium compound 3 is only 51 Å³.

Collection and Reduction of X-ray Data. Details of intensity data collection for all three compounds are presented in Table II. All three data sets were collected at 295 ± 1 K on a Syntex P2₁ diffractometer using graphite-monochromated Mo K α (λ = 0.71069 Å) radiation and θ -2 θ scans with a variable scan rate set to optimize measurements of weak reflections. Background

Table III. Atomic Positions (Fractional $\times 10^4$) and Hydrogen Atom Thermal Parameters ($\times 10^3$) for $(\mu\text{-H})_2\text{Fe}_3(\text{CO})_8(\mu\text{-PPH}_2)_2$

A. Heavy Atoms							
atom	x	y	z	atom	x	y	z
Fe(1)	2133.9 (5)	1171.7 (5)	1169.2 (4)	C(13)	2944 (4)	-1399 (5)	6301 (3)
Fe(2)	1145.2 (5)	647.9 (4)	2894.9 (4)	C(14)	2799 (4)	-0849 (4)	5349 (3)
Fe(3)	3467.4 (5)	944.7 (5)	2799.3 (4)	C(15)	3633 (4)	-2096 (3)	2885 (3)
P(1)	2960.5 (9)	-795.3 (8)	3426.9 (7)	C(16)	2839 (5)	-2570 (4)	2525 (3)
P(2)	322.7 (9)	2316.1 (8)	1775.1 (7)	C(17)	3348 (6)	-3564 (4)	2127 (4)
O(1)	4431 (3)	-783 (3)	787 (2)	C(18)	4658 (6)	-4081 (5)	2069 (4)
O(2)	785 (3)	975 (3)	-381 (2)	C(19)	5467 (5)	-3627 (4)	2412 (4)
O(3)	3061 (3)	3072 (3)	-83 (2)	C(20)	4967 (4)	-2647 (4)	2835 (4)
O(4)	-462 (3)	-917 (3)	3074 (2)	C(21)	-1227 (3)	2592 (3)	1239 (2)
O(5)	-77 (3)	1427 (3)	4564 (2)	C(22)	-1568 (4)	1602 (4)	1137 (3)
O(6)	6115 (3)	-278 (3)	2265 (3)	C(23)	-2725 (4)	1783 (4)	725 (3)
O(7)	4070 (3)	1321 (3)	4575 (3)	C(24)	-3556 (4)	2956 (4)	385 (3)
O(8)	3569 (3)	3420 (3)	1893 (3)	C(25)	-3222 (4)	3935 (4)	478 (3)
C(1)	3573 (4)	-46 (4)	997 (3)	C(26)	-2081 (4)	3770 (3)	898 (3)
C(2)	1271 (4)	1041 (3)	248 (3)	C(27)	141 (4)	3846 (3)	1921 (3)
C(3)	2695 (4)	2356 (3)	436 (3)	C(28)	555 (4)	4677 (4)	1240 (3)
C(4)	162 (4)	-90 (3)	2978 (3)	C(29)	289 (5)	5882 (4)	1324 (4)
C(5)	404 (4)	1122 (3)	3907 (3)	C(30)	-379 (5)	6225 (4)	2085 (4)
C(6)	5071 (4)	191 (4)	2461 (4)	C(31)	-812 (6)	5410 (4)	2770 (4)
C(7)	3841 (4)	1131 (4)	3891 (3)	C(32)	-543 (5)	4205 (4)	2684 (3)
C(8)	3472 (4)	2469 (4)	2204 (3)	C(33) ^a	-501 (14)	4046 (9)	5312 (6)
C(9)	3180 (4)	-1535 (3)	4676 (3)	C(34) ^a	758 (15)	3751 (9)	5039 (6)
C(10)	3711 (5)	-2802 (4)	5004 (3)	C(35) ^a	1364 (14)	4724 (11)	4693 (6)
C(11)	3849 (7)	-3337 (5)	5955 (4)	C(36) ^a	2428 (19)	4448 (22)	4464 (17)
C(12)	3478 (5)	-2644 (5)	6604 (4)				

B. Hydrogen Atom Positions (Fractional $\times 10^3$) and Isotropic Temperature Factors									
atom	x	y	z	$U_{\text{iso}}, \text{\AA}^2$	atom	x	y	z	$U_{\text{iso}}, \text{\AA}^2$
H(1)	168 (4)	22 (4)	199 (3)	65 (12)	H(20)	550 (4)	-230 (4)	311 (3)	64 (14)
H(2)	200 (3)	157 (3)	297 (2)	48 (10)	H(22)	-103 (3)	83 (3)	134 (3)	48 (10)
H(10)	395 (4)	-319 (4)	448 (3)	89 (15)	H(23)	-298 (4)	110 (4)	72 (3)	69 (14)
H(11)	424 (5)	-422 (5)	615 (4)	115 (19)	H(24)	-434 (4)	304 (4)	11 (3)	57 (12)
H(12)	349 (4)	-302 (4)	731 (3)	89 (14)	H(25)	-378 (4)	479 (4)	19 (3)	65 (13)
H(13)	267 (4)	-87 (4)	678 (3)	72 (14)	H(26)	-184 (4)	446 (4)	98 (3)	62 (13)
H(14)	239 (4)	-4 (4)	514 (3)	71 (14)	H(28)	95 (4)	447 (4)	67 (3)	60 (12)
H(16)	194 (4)	-217 (4)	251 (3)	61 (14)	H(29)	58 (4)	643 (4)	80 (3)	75 (15)
H(17)	273 (5)	-385 (4)	176 (4)	100 (18)	H(30)	-55 (5)	701 (5)	216 (4)	116 (18)
H(18)	502 (5)	-468 (5)	171 (4)	105 (18)	H(31)	-124 (5)	563 (4)	329 (4)	90 (16)
H(19)	636 (5)	-396 (4)	239 (3)	90 (16)	H(32)	-88 (4)	371 (4)	316 (3)	53 (12)

^a Represents the disordered toluene of crystallization.

measurements, using the stationary crystal-stationary counter method, were made at the beginning and end of each scan. Two standard reflections monitored after every 100 intensity measurements showed no significant changes ($\leq 2\%$) for 1 and 2 but decreased by 9% for 3. These were used to scale the data to a common level. Measured reflections were flagged as unobserved when $I \leq 3\sigma(I)$ where σ was derived from counting statistics. Lorentz and polarization corrections were applied to the three data sets. A spherical absorption correction was made for 3.¹⁵

Solution and Refinement of Intensity Data. A Patterson synthesis for the iron compound readily yielded positions for the three metal atoms. Standard Fourier methods were used to locate the remaining atoms in the molecule including a disordered solvent molecule (toluene) located on a centre of symmetry at $0, \frac{1}{2}, \frac{1}{2}$. Full-matrix least-squares refinements of positional and isotropic thermal parameters gave an R value ($R = \sum |F_o| - |F_c| / \sum |F_o|$) of 0.091. Conversion to anisotropic coefficients for all non-hydrogen atoms and several further cycles of refinement gave $R = 0.046$. At this stage a difference Fourier map revealed the positions of all hydrogen atoms including the two bridging hydrogen atoms across the Fe(1)-Fe(2) and Fe(2)-Fe(3) vectors. In subsequent refinements to convergence hydrogen atom positions and isotropic temperature coefficients were included. The function minimized in least-squares calculations was $\sum w(|F_o| - |F_c|)^2$. The weighted R value is defined as $R_w = [\sum w(|F_o| - |F_c|)^2 / \sum w|F_o|^2]^{1/2}$ where the weights w , which optimize on moderate intensities, were taken from the program RANGER. Scattering factors were taken from

the ref 15a, and corrections for anomalous dispersion by the metal atoms were applied. Scattering factors for hydrogen were taken from the data of Stewart et al.^{15b} The final R and R_w values together with residual electron density maxima are given in Table II.

For the corresponding ruthenium and osmium compounds 2 and 3, atomic positions were allocated from the refined iron molecule coordinates and refinement proceeded smoothly as indicated in Table III confirming the isomorphism of the crystalline forms of 1, 2, and 3. Hydrogen atoms were not included in the refinement of 3.

All calculations were carried out of an IBM 4341 network in the University of Waterloo Computing Centre, using a package of programs already described.¹⁶ Atomic positional parameters for 1-3 are listed in Tables III-V while Table VI contains an appropriate selection of bond lengths and angles. Anisotropic thermal parameters (Tables S1-S3), remaining bond lengths and angles (Table S4), and structure factors (Table S5-S7) have been deposited as supplementary material.

Results and Discussion

Synthesis and Spectroscopic Characterization of $(\mu\text{-H})_2\text{M}_3(\text{CO})_8(\mu\text{-PPH}_2)_2$. The oxidative addition of P-H bonds in primary and secondary phosphines to metal carbonyls has been successfully used for the synthesis of a number of diorganophosphido (R_2P) and phosphinidene (RP) based polynuclear compounds.¹⁷ A shortcoming of

(15) (a) "International Tables for X-ray Crystallography"; Kynoch Press; Birmingham, England, 1974. (b) Stewart, R. F.; Davidson, E. R.; Simpson, W. T. *J. Chem. Phys.* **1965**, *42*, 3175.

(16) Carty, A. J.; Mott, G. N.; Taylor, N. J.; Yule, J. E. *J. Am. Chem. Soc.* **1978**, *100*, 3051.

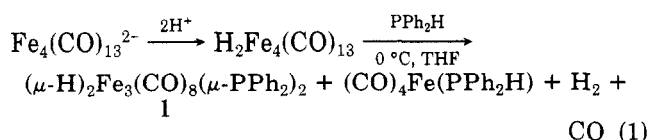
Table IV. Atomic Positions (Fractional $\times 10^4$) and Hydrogen Atom Thermal Parameters for $(\mu\text{-H})_2\text{Ru}_3(\text{CO})_8(\mu\text{-PPh}_2)_2$

A. Heavy Atoms							
atom	x	y	z	atom	x	y	z
Ru(1)	2128.9 (2)	1152.6 (2)	1095.2 (2)	C(13)	2992 (4)	-1408 (4)	6313 (3)
Ru(2)	1037.5 (2)	629.2 (2)	2930.0 (2)	C(14)	2831 (3)	-877 (3)	5373 (2)
Ru(3)	3477.5 (2)	964.2 (2)	2787.2 (2)	C(15)	3631 (3)	-2140 (3)	2902 (2)
P(1)	2969.8 (7)	-847.2 (2)	3453.3 (6)	C(16)	2842 (4)	-2622 (3)	2573 (3)
P(2)	234.4 (7)	2369.5 (7)	1744.6 (5)	C(17)	3358 (5)	-3627 (4)	2170 (3)
O(1)	4518 (3)	-913 (2)	749 (2)	C(18)	4642 (5)	-4128 (4)	2080 (3)
O(2)	692 (3)	1010 (2)	-512 (2)	C(19)	5428 (4)	-3659 (4)	2390 (3)
O(3)	3101 (3)	3085 (2)	-168 (2)	C(20)	4944 (4)	-2672 (3)	2814 (3)
O(4)	-606 (3)	-940 (2)	3040 (2)	C(21)	-1279 (3)	2652 (3)	1193 (2)
O(5)	-182 (2)	1420 (2)	4689 (2)	C(22)	-1613 (3)	1668 (3)	1100 (2)
O(6)	6187 (3)	-300 (3)	2176 (3)	C(23)	-2747 (4)	1843 (4)	683 (3)
O(7)	4104 (3)	1025 (3)	4646 (2)	C(24)	-3555 (4)	2997 (4)	348 (3)
O(8)	3517 (3)	3515 (2)	1831 (2)	C(25)	-3235 (3)	3978 (3)	427 (3)
C(1)	3658 (3)	-162 (3)	920 (2)	C(26)	-2110 (3)	3810 (3)	854 (2)
C(2)	1198 (3)	1058 (3)	106 (2)	C(27)	50 (3)	3874 (3)	1909 (2)
C(3)	2735 (3)	2382 (3)	319 (2)	C(28)	510 (3)	4677 (3)	1254 (3)
C(4)	-10 (3)	-326 (3)	2985 (2)	C(29)	269 (4)	5852 (3)	1354 (3)
C(5)	260 (3)	1117 (3)	4030 (2)	C(30)	-413 (4)	6218 (3)	2114 (3)
C(6)	5174 (4)	175 (3)	2391 (3)	C(31)	-873 (5)	5437 (4)	2765 (3)
C(7)	3903 (3)	1138 (3)	3966 (3)	C(32)	-645 (4)	4262 (3)	2668 (3)
C(8)	3460 (3)	2580 (3)	2157 (3)	C(33) ^a	-446 (13)	4054 (8)	5291 (5)
C(8)	3221 (3)	-1564 (3)	4698 (2)	C(34) ^a	723 (15)	3772 (9)	5001 (6)
C(10)	3753 (5)	-2809 (4)	5015 (3)	C(35) ^a	1259 (13)	4756 (10)	4680 (6)
C(11)	3900 (6)	-3326 (4)	5963 (3)	C(36) ^a	2252 (17)	4413 (19)	4454 (14)
C(12)	3520 (5)	-2633 (5)	6605 (3)				

B. Hydrogen Atom Positions ($\times 10^3$) and Isotropic Temperature Factors									
atom	x	y	z	$U_{\text{iso}}, \text{\AA}^2$	atom	x	y	z	$U_{\text{iso}}, \text{\AA}^2$
H(1)	172 (4)	10 (4)	185 (3)	86 (15)	H(20)	545 (3)	-243 (3)	306 (2)	48 (10)
H(2)	193 (4)	171 (4)	304 (3)	58 (12)	H(22)	-106 (3)	86 (3)	132 (2)	40 (7)
H(10)	401 (4)	-328 (4)	463 (3)	68 (12)	H(23)	-292 (3)	117 (3)	61 (3)	49 (11)
H(11)	433 (5)	-415 (5)	616 (3)	97 (16)	H(24)	-426 (4)	313 (3)	8 (3)	64 (11)
H(12)	363 (4)	-296 (4)	724 (3)	68 (12)	H(25)	-383 (3)	479 (3)	16 (2)	48 (9)
H(13)	273 (3)	-96 (3)	672 (2)	46 (9)	H(26)	-190 (3)	443 (3)	94 (2)	47 (10)
H(14)	252 (2)	-7 (3)	520 (2)	38 (7)	H(28)	101 (4)	437 (3)	74 (3)	70 (11)
H(16)	192 (4)	-229 (3)	262 (3)	64 (12)	H(29)	62 (4)	638 (4)	93 (3)	62 (12)
H(17)	283 (4)	-397 (4)	193 (3)	87 (14)	H(30)	-64 (4)	704 (4)	216 (3)	90 (14)
H(18)	497 (3)	-484 (3)	178 (3)	62 (10)	H(31)	-134 (4)	566 (4)	327 (3)	77 (12)
H(19)	632 (4)	-307 (4)	234 (3)	73 (13)	H(32)	-98 (3)	375 (3)	304 (2)	46 (9)

^a See footnote a in Table III.

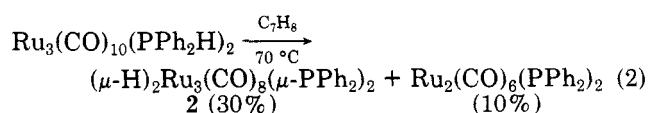
this method is that the thermal or photochemical activation frequently needed to effect P-H bond cleavage may lead to fragmentation of the metal carbonyl precursor and low yields of the desired polynuclear cluster. Thus reaction of $\text{Fe}_3(\text{CO})_{12}$ with PPh_2H did not appear to be an attractive route to $(\mu\text{-H})_2\text{Fe}_3(\text{CO})_8(\mu\text{-PPh}_2)_2$ since the corresponding reaction with PMe_2H afforded only very low yields of the dimethylphosphido-bridged species.⁴ We have adopted an alternative strategy involving controlled degradation of a higher nuclearity hydridoiron cluster, with hydrogen elimination in the presence of diphenylphosphine to synthesize the molecule $(\mu\text{-H})_2\text{Fe}_3(\text{CO})_8(\mu\text{-PPh}_2)_2$ (eq 1).



Treatment of a slurry of the PPN^+ salt of the known tetranuclear anion $\text{Fe}_4(\text{CO})_{13}^{2-}$ with CF_3COOH in the presence of 3 equiv of PPh_2H at 0 °C rapidly gave a brown solution which turned green on warming to room temperature. The desired product, dark green **1**, was obtained

in ~60% yield after chromatography together with a yellow mononuclear compound readily identified as $\text{Fe}(\text{CO})_4(\text{PPh}_2\text{H})$ by IR spectroscopy.¹² In the absence of CF_3COOH , treatment of $\text{Fe}_4(\text{CO})_{13}^{2-}$ did not lead to **1**; thus it seems likely that elimination of dihydrogen from the intermediate $\text{H}_2\text{Fe}_4(\text{CO})_{13}$ (or possibly $\text{HF}_4(\text{CO})_{13}^-$) on reaction with PPh_2H generates the phosphido groups. There is ample precedent for hydrogen elimination in reactions of metal carbonyls with primary or secondary phosphines in other systems.¹⁸

Previous studies with phosphido-bridged ruthenium clusters, notably the synthesis of $(\mu\text{-H})\text{Ru}_3(\text{CO})_{10}(\mu\text{-PPh}_2)$ and $(\mu\text{-H})\text{Ru}_3(\text{CO})_9(\mu\text{-PPh}_2)$,⁹ led us to believe that under appropriate conditions $(\mu\text{-H})_2\text{Ru}_3(\text{CO})_8(\mu\text{-PPh}_2)_2$ might be accessible via the controlled intramolecular oxidative cleavage of P-H bonds in $\text{Ru}_3(\text{CO})_{10}(\text{PPh}_2\text{H})_2$. The latter was prepared in 38% yield from $\text{Ru}_3(\text{CO})_{12}$ via the radical-initiated substitution method¹³ and thermolyzed at 70 °C in toluene (eq 2) affording moderate but workable



yields of **2**. The osmium cluster **3** was obtained in good yields via the pyrolysis of $\text{Os}_3(\text{CO})_{10}(\text{PPh}_2\text{H})_2$, synthesized

(17) See, for example: (a) Hayter, R. G. In "Preparative Inorganic Reactions"; Jolly, W. L., Ed.; Interscience: New York, 1965; p 211. (b) Huttner, G.; Schneider, J.; Mohr, G.; Von Seyerl, J. *J. Organomet. Chem.* **1980**, *191*, 161. (c) Field, J. S.; Haines, R. J.; Smit, D. N.; Natarajan, K.; Scheidsteger, O.; Huttner, G. *J. Organomet. Chem.* **1982**, *240*, C23. (d) Vahrenkamp, H.; Wolters, D. *J. Organomet. Chem.* **1982**, *224*, C17.

(18) (a) Vahrenkamp, H.; Wucherer, E. J. *Angew. Chem., Int. Ed. Engl.* **1981**, *20*, 680. (b) Harley, D.; Whittle, R. R.; Geoffroy, G. L. *Organometallics* **1983**, *2*, 60.

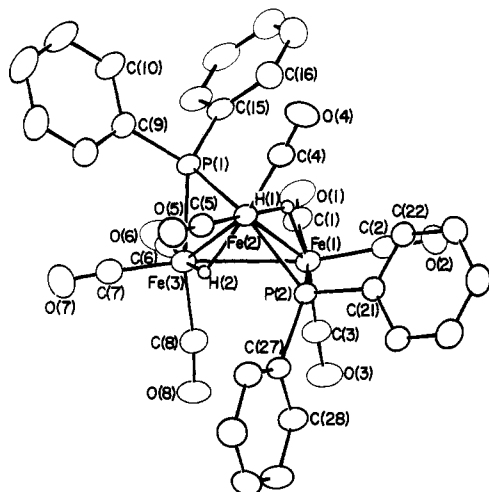
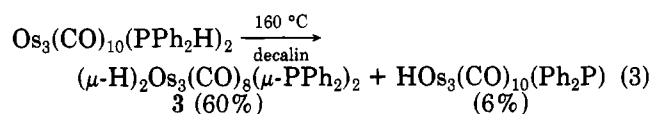
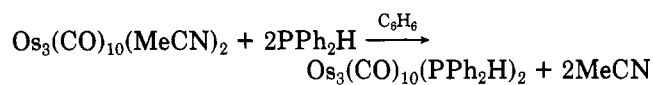
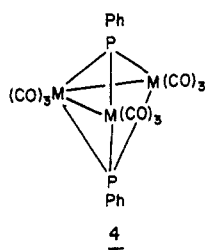
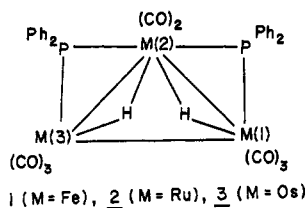


Figure 1. An ORTEP view of the molecular structure of $(\mu\text{-H})_2\text{Fe}_3(\text{CO})_8(\mu\text{-PPh}_2)_2$ showing the atomic numbering used for 1, 2, and 3.

by the displacement of MeCN from $\text{Os}_3(\text{CO})_{10}(\text{MeCN})_2$ by PPh_2H (eq 3).



The three clusters 1–3 have been characterized spectroscopically and by single-crystal X-ray diffraction (vide infra). Only terminal $\nu(\text{CO})$ bands appear in the solution IR spectra and triplet NMR resonances are present at high field in the proton NMR spectra with apparent $^2J_{\text{P-H}}$ values which decrease from 41.8 Hz for 1 to 23.0 Hz for 2 and 13.7 Hz for 3. The high field hydride resonances



do not exhibit any temperature dependence over the range -50 to $+60$ $^\circ\text{C}$, indicating that the molecules are either nonfluxional in this temperature regime or alternatively undergoing a very fast rearrangement on the NMR time scale. The triplet ^1H and ^{31}P resonances are consistent with equivalent phosphorus atoms and equivalent hydrogen atoms or with deceptively simple AA'XX' spectra.¹⁹ The X-ray structure analyses clearly indicate the near equivalence of the two phosphorus atoms P(1) and P(2)

(19) A similar problem arises with the spectrum of the corresponding $(\mu\text{-H})_2\text{Fe}_3(\text{CO})_8(\mu\text{-PMe}_2)_2$ compound.⁴

Table V. Atomic Positions (Fractional $\times 10^4$) for $(\mu\text{-H})_2\text{Os}_3(\text{CO})_8(\mu\text{-PPh}_2)_2$

atom	x	y	z
Os(1)	2133.1 (3)	1144.9 (3)	1084.6 (2)
Os(2)	1023.6 (3)	634.5 (3)	2933.9 (2)
Os(3)	3462.6 (3)	996.2 (3)	2787.5 (3)
P(1)	2967 (2)	-838 (2)	3465 (2)
P(2)	220 (2)	2381 (2)	1737 (2)
O(1)	4532 (8)	-932 (7)	732 (6)
O(2)	692 (9)	1017 (7)	-529 (6)
O(3)	3112 (9)	3079 (7)	-159 (6)
O(4)	-625 (8)	-920 (7)	3026 (7)
O(5)	-193 (8)	1401 (7)	4713 (5)
O(6)	6159 (8)	-248 (9)	2128 (8)
O(7)	4134 (8)	1321 (8)	4654 (6)
O(8)	3498 (10)	3541 (8)	1821 (7)
C(1)	3643 (11)	-181 (10)	894 (8)
C(2)	1209 (10)	1059 (9)	93 (7)
C(3)	2745 (10)	2371 (9)	320 (8)
C(4)	-14 (9)	-316 (9)	2986 (7)
C(5)	257 (9)	1093 (9)	4039 (7)
C(6)	5139 (11)	214 (12)	2356 (9)
C(7)	3913 (10)	1154 (9)	3964 (8)
C(8)	3430 (12)	2622 (10)	2159 (7)
C(9)	3216 (9)	-1542 (9)	4715 (7)
C(10)	3788 (14)	-2807 (11)	5010 (8)
C(11)	3901 (17)	-3348 (13)	5971 (9)
C(12)	3538 (13)	-2612 (14)	6630 (9)
C(13)	2989 (11)	-1387 (12)	6333 (8)
C(14)	2822 (10)	-841 (10)	5379 (7)
C(15)	3598 (9)	-2126 (8)	2898 (7)
C(16)	2832 (11)	-2626 (10)	2392 (8)
C(17)	3357 (14)	-3639 (11)	2181 (9)
C(18)	4644 (14)	-4119 (11)	2075 (9)
C(19)	5447 (12)	-3633 (11)	2383 (9)
C(20)	4956 (11)	-2651 (10)	2815 (8)
C(21)	-1284 (8)	2667 (8)	1172 (6)
C(22)	-1602 (11)	1663 (9)	1092 (8)
C(23)	-2751 (11)	1843 (10)	683 (8)
C(24)	-3571 (10)	3024 (11)	331 (8)
C(25)	-3240 (10)	4005 (9)	411 (8)
C(26)	-2108 (9)	3831 (9)	855 (7)
C(27)	59 (9)	3879 (8)	1899 (7)
C(28)	515 (10)	4679 (9)	1247 (8)
C(29)	287 (13)	5862 (11)	1347 (10)
C(30)	-415 (14)	6244 (10)	2113 (9)
C(31)	-902 (14)	5446 (12)	2778 (8)
C(32)	-660 (12)	4255 (10)	2688 (8)
C(33) ^a	-483 (43)	4037 (25)	5319 (17)
C(34) ^a	617 (47)	3783 (30)	5007 (19)
C(35) ^a	1278 (41)	4752 (32)	4679 (17)
C(36) ^a	2248 (58)	4378 (59)	4440 (44)

^a See footnote a in Table III.

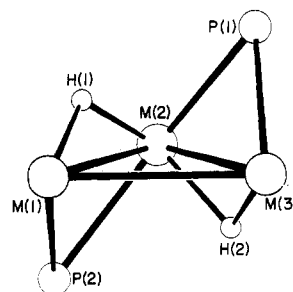


Figure 2. A perspective view of the skeleton of $(\mu\text{-H})_2\text{Fe}_3(\text{CO})_8(\mu\text{-PPh}_2)_2$ with the phenyl rings and carbonyls removed for clarity.

with respect to H(1) and H(2), and it is this symmetry which presumably gives rise to the observed spectra. The ^{31}P chemical shifts of the $\mu\text{-PPh}_2$ groups are well downfield of 85% H_3PO_4 as expected for phosphido bridges across a metal-metal bond.²⁰ The upfield shift of $\delta(^{31}\text{P})$ from

(20) See, for example, ref 1i and: Mott, G. N.; Carty, A. J. *Inorg. Chem.* 1983, 22, 2786.

Table VI. A Selection of Bond Lengths (Å) and Bond Angles (deg) for $(\mu\text{-H})_2\text{M}_3(\text{CO})_8(\mu\text{-PPh}_2)_2$

A. Bond Lengths							
	M = Fe	M = Ru	M = Os		M = Fe	M = Ru	M = Os
M(1)–M(2)	2.6670 (8)	2.8700 (3)	2.8928 (4)	M(2)–H(1)	1.54 (4)	1.85 (5)	
M(1)–M(3)	2.8264 (8)	2.9464 (3)	2.9601 (5)	M(2)–H(2)	1.69 (4)	1.92 (4)	
M(2)–M(3)	2.6588 (8)	2.8642 (3)	2.8864 (5)	M(3)–H(2)	1.55 (4)	1.71 (5)	
M(1)–P(2)	2.257 (1)	2.3930 (8)	2.413 (2)	P(1)–C(9)	1.820 (4)	1.827 (3)	1.827 (10)
M(2)–P(2)	2.207 (1)	2.3403 (8)	2.349 (2)	P(1)–C(15)	1.832 (4)	1.828 (3)	1.825 (10)
M(2)–P(1)	2.201 (1)	2.3338 (8)	2.341 (3)	P(2)–C(21)	1.828 (4)	1.831 (3)	1.833 (10)
M(3)–P(1)	2.262 (1)	2.3929 (8)	2.412 (3)	P(2)–C(27)	1.832 (4)	1.824 (3)	1.814 (10)
M(1)–C(1)	1.804 (4)	1.940 (4)	1.935 (12)	C(1)–O(1)	1.136 (5)	1.131 (4)	1.132 (15)
M(1)–C(2)	1.786 (4)	1.908 (4)	1.901 (11)	C(2)–O(2)	1.139 (5)	1.135 (5)	1.142 (14)
M(1)–C(3)	1.783 (4)	1.914 (4)	1.909 (11)	C(3)–O(3)	1.141 (5)	1.131 (5)	1.132 (15)
M(2)–C(4)	1.762 (4)	1.880 (3)	1.870 (11)	C(4)–O(4)	1.141 (5)	1.134 (4)	1.144 (14)
M(2)–C(5)	1.760 (4)	1.887 (3)	1.874 (10)	C(5)–O(5)	1.142 (5)	1.129 (4)	1.150 (12)
M(3)–C(6)	1.777 (5)	1.915 (4)	1.913 (13)	C(6)–O(6)	1.140 (6)	1.134 (5)	1.143 (17)
M(3)–C(7)	1.777 (4)	1.914 (4)	1.910 (11)	C(7)–O(7)	1.151 (6)	1.133 (5)	1.139 (14)
M(3)–C(8)	1.800 (4)	1.935 (4)	1.936 (12)	C(8)–O(8)	1.141 (6)	1.132 (5)	1.120 (15)
M(1)–H(1)	1.59 (4)	1.64 (5)					

B. Bond Angles							
	M = Fe	M = Ru	M = Os		M = Fe	M = Ru	M = Os
M(2)–M(1)–M(3)	57.81 (1)	58.98 (1)	59.08 (1)	C(5)–M(2)–H(1)	175 (2)	176 (2)	
M(2)–M(1)–P(2)	52.45 (2)	51.84 (1)	51.59 (5)	C(5)–M(2)–H(2)	81 (1)	80 (1)	
M(2)–M(1)–C(1)	111.5 (1)	111.3 (1)	112.0 (3)	H(1)–M(2)–H(2)	103 (2)	104 (2)	
M(2)–M(1)–C(2)	115.5 (1)	114.4 (1)	114.5 (3)	M(1)–M(3)–M(2)	58.09 (1)	59.18 (1)	59.30 (1)
M(2)–M(1)–C(3)	138.3 (1)	139.0 (1)	138.5 (3)	M(1)–M(3)–P(1)	87.13 (2)	87.21 (2)	86.92 (6)
M(2)–M(1)–H(1)	31 (1)	37 (2)		M(1)–N(7)–C(6)	99.3 (1)	98.2 (1)	96.0 (4)
M(3)–M(1)–P(2)	88.39 (2)	88.02 (1)	87.53 (5)	M(1)–M(3)–C(7)	162.2 (1)	164.1 (1)	165.7 (3)
M(3)–M(1)–C(1)	82.4 (1)	82.3 (1)	84.0 (3)	M(1)–M(3)–C(8)	82.7 (1)	83.0 (1)	83.6 (3)
M(3)–M(1)–C(2)	169.4 (1)	171.2 (1)	172.0 (3)	M(1)–M(3)–H(2)	73 (1)	77 (1)	
M(3)–M(1)–C(3)	95.9 (1)	95.2 (1)	94.2 (3)	M(2)–M(3)–P(1)	52.40 (2)	51.77 (2)	51.49 (6)
M(3)–M(1)–H(1)	74 (1)	78 (2)		M(2)–M(3)–C(6)	137.8 (1)	138.1 (1)	136.9 (4)
P(2)–M(1)–C(1)	163.9 (1)	163.1 (1)	163.4 (3)	M(2)–M(3)–C(7)	110.1 (1)	109.8 (1)	110.5 (3)
P(2)–M(1)–C(2)	93.1 (1)	91.8 (1)	91.5 (3)	M(2)–M(3)–C(8)	113.9 (1)	114.4 (1)	114.6 (3)
P(2)–M(1)–C(3)	100.0 (1)	100.7 (1)	100.8 (3)	M(2)–M(3)–H(2)	37 (1)	41 (1)	
P(2)–M(1)–H(1)	75 (1)	80 (2)		P(1)–M(3)–C(6)	95.3 (1)	96.3 (1)	96.5 (4)
C(1)–M(1)–C(2)	93.6 (1)	95.7 (1)	94.9 (4)	P(1)–M(3)–C(7)	95.4 (1)	94.1 (1)	93.8 (3)
C(1)–M(1)–C(3)	94.1 (1)	93.9 (1)	94.0 (4)	P(1)–M(3)–C(8)	166.2 (1)	166.1 (1)	166.1 (3e)
C(1)–M(1)–H(1)	90 (1)	85 (2)		P(1)–M(3)–H(2)	83 (1)	85 (1)	
C(2)–M(1)–C(3)	94.2 (1)	93.6 (1)	93.8 (4)	C(6)–M(3)–C(7)	98.0 (2)	97.5 (1)	98.1 (5)
C(2)–M(1)–H(1)	97 (1)	93 (2)		C(6)–M(3)–C(8)	95.6 (2)	94.9 (1)	94.6 (5)
C(3)–M(1)–H(1)	168 (1)	174 (2)		C(6)–M(3)–H(2)	172 (1)	175 (1)	
M(1)–M(2)–M(3)	64.10 (1)	61.84 (1)	61.62 (1)	C(7)–M(3)–C(8)	91.5 (2)	92.7 (1)	93.0 (4)
M(1)–M(2)–P(1)	92.46 (2)	90.15 (2)	89.85 (6)	C(7)–M(3)–H(2)	90 (1)	87 (1)	
M(1)–M(2)–P(2)	54.18 (2)	53.51 (1)	53.60 (5)	C(8)–M(3)–H(2)	85 (1)	83 (1)	
M(1)–M(2)–C(4)	112.1 (1)	112.0 (1)	112.0 (3)	M(2)–P(1)–M(3)	73.12 (2)	74.58 (2)	74.78 (6)
M(1)–M(2)–C(5)	149.8 (1)	150.7 (1)	152.0 (3)	M(2)–P(1)–C(9)	121.2 (1)	120.8 (1)	120.6 (3)
M(1)–M(2)–H(1)	32 (1)	32 (2)		M(2)–P(1)–C(15)	120.0 (1)	119.5 (1)	117.8 (3)
M(1)–M(2)–H(2)	76 (1)	76 (1)		M(3)–P(1)–C(9)	120.9 (1)	120.7 (1)	120.5 (3)
M(3)–M(2)–P(1)	54.48 (2)	53.65 (2)	53.74 (6)	M(3)–P(1)–C(15)	118.9 (1)	118.7 (1)	118.8 (3)
M(3)–M(2)–P(2)	93.83 (2)	91.02 (1)	90.50 (5)	C(9)–P(1)–C(15)	102.3 (1)	102.3 (1)	103.6 (4)
M(3)–M(2)–C(4)	150.9 (1)	152.2 (1)	152.8 (3)	M(1)–P(2)–M(2)	73.37 (2)	74.65 (1)	74.81 (5)
M(3)–M(2)–C(5)	105.0 (1)	106.0 (1)	106.1 (3)	M(1)–P(2)–C(21)	117.8 (1)	117.3 (1)	117.1 (2)
M(3)–M(2)–H(1)	80 (1)	78 (2)		M(1)–P(2)–C(27)	122.6 (1)	122.7 (1)	121.7 (3)
M(3)–M(2)–H(2)	33 (1)	35 (1)		M(2)–P(2)–C(21)	120.5 (1)	119.7 (1)	120.0 (2)
P(1)–M(2)–P(2)	143.63 (3)	140.23 (2)	139.85 (8)	M(2)–P(2)–C(27)	121.6 (1)	121.5 (1)	121.1 (3)
P(1)–M(2)–C(4)	98.5 (1)	101.4 (1)	102.0 (3)	C(21)–P(2)–C(27)	101.0 (1)	101.2 (1)	102.0 (4)
P(1)–M(2)–C(5)	103.7 (1)	103.7 (1)	102.7 (3)	M(1)–C(1)–O(1)	172.1 (1)	174.7 (1)	176.3 (4)
P(1)–M(2)–H(1)	79 (1)	78 (2)		M(1)–C(2)–O(2)	175.4 (1)	176.5 (1)	177.1 (4)
P(1)–M(2)–H(2)	82 (1)	83 (1)		M(1)–C(3)–O(3)	175.1 (1)	177.2 (1)	177.6 (4)
P(2)–M(2)–C(4)	106.9 (1)	106.8 (1)	106.7 (3)	M(2)–C(4)–O(4)	176.9 (1)	177.1 (1)	178.4 (4)
P(2)–M(2)–C(5)	101.5 (1)	103.7 (1)	104.7 (3)	M(2)–C(5)–O(5)	179.8 (1)	178.2 (1)	177.7 (4)
P(2)–M(2)–H(1)	78 (1)	77 (2)		M(3)–C(6)–O(6)	177.7 (2)	178.6 (1)	177.3 (5)
P(2)–M(2)–H(2)	76 (1)	83 (1)		M(3)–C(7)–O(7)	176.2 (1)	175.1 (1)	175.8 (4)
C(4)–M(2)–C(5)	90.9 (1)	90.7 (1)	90.0 (4)	M(3)–C(8)–O(8)	173.0 (1)	175.0 (1)	174.8 (5)
C(4)–M(2)–H(1)	85 (2)	85 (2)		M(1)–H(1)–M(2)	117 (1)	110 (1)	
C(4)–M(2)–H(2)	172 (1)	170 (1)		M(2)–H(2)–M(3)	110 (1)	104 (1)	

Fe → Os follows the usual trend in paramagnetic shielding for this triad.¹¹

Crystal and Molecular Structures of $(\mu\text{-H})_2\text{M}_3(\text{CO})_8(\mu\text{-PPh}_2)_2$. Compounds 1–3 are isostructural. A perspective view of one molecule drawn to illustrate the mutual disposition of the bridging ligands is shown in Figure 1. The molecules consist of a triangular core of metal atoms with the M(1)–M(2) and M(2)–M(3) edges

each bridged by $\mu\text{-PPh}_2$ and $\mu\text{-H}$ ligands. The geometry of this skeleton is better illustrated in Figure 2 where carbonyl ligands and phenyl groups have been removed and the stereochemistry of the remaining atoms emphasized. It is clear that the two phosphido groups lie respectively above and below the trimetal plane; P(1) occupies an axial site on M(3) while P(2) is axial on M(1). With respect to the unique iron atom Fe(2), P(1) and P(2) are

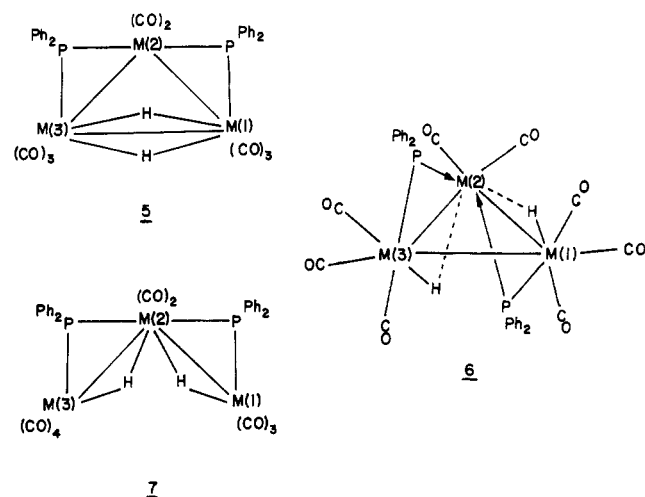
approximately trans to one another [P(1)–M(2)–P(2) = 143.6 (1)°, 1, 140.2 (1)°, 2, and 139.9 (1)°, 3] and cis to the two bridging hydrides [e.g., P(1)–Fe(2)–H(2) = 82 (1)°; P(1)–Fe(2)–H(1) = 79 (1)°; P(2)–Fe(2)–H(2) = 76 (1)°; P(2)–Fe(2)–H(1) = 78 (1)°]. Thus the stereochemistry of the central metal atom in each case is distorted octahedral provided that the two metal–metal vectors are ignored. This mutual anti relationship of two bridging phosphido groups on a trimetal framework is not limited to this series. Similar stereochemical relationships have been found in the molecules $\text{FeCO}_2(\text{CO})_7(\mu\text{-CO})(\mu\text{-PPh}_2)_2$,²¹ $\text{Co}_3(\text{CO})_6(\mu\text{-CO})(\mu\text{-PPh}_2)_2$,²² $(\mu\text{-H})_2\text{Fe}_3(\text{CO})_8(\mu\text{-PMe}_2)_2$,⁴ and $\text{RuCO}_2(\text{CO})_7(\mu\text{-CO})(\mu\text{-PPh}_2)_2$ ²³ and can clearly be attributed to the unfavorable steric interactions between phenyl groups which might arise for syn arrangements of PPh_2 groups on a triangular skeleton. Although there is no crystallographically imposed symmetry, the mutual arrangement of ligands confers an approximate twofold axis of symmetry on the individual molecules 1–3 with the axis bisecting the angle C(4)–M(2)–C(5).

For 1 all three Fe–Fe interactions are bonding [Fe(1)–Fe(2) = 2.6670 (8); Fe(2)–Fe(3) = 2.6588 (8), and Fe(1)–Fe(3) = 2.8264 (8) Å] and define a nearly isosceles triangle. This is also reflected by the angles subtended at the iron atoms within the trimetallic framework [Fe(1)–Fe(2)–Fe(3) = 64.1°; Fe(2)–Fe(1)–Fe(3) = 57.8°; Fe(2)–Fe(3)–Fe(1) = 58.1°]. The Fe–Fe bond lengths in 1 compare well with those in the closely related $\mu\text{-PMe}_2$ -bridged compound [$(\mu\text{-H})_2\text{Fe}_3(\text{CO})_8(\mu\text{-PMe}_2)_2$] [Fe–Fe = 2.645 (av) and 2.826 Å].⁴ While the two short Fe–Fe bond lengths are well within the range normally found for Fe–Fe single bonds in other homonuclear iron clusters [e.g., $\text{Fe}_3(\text{CO})_{12}$,²⁴ 2.558 (1)–2.683 (1) Å; $\text{HFe}_3(\text{CO})_9(\text{CH}_3\text{C}=\text{NH})$,²⁵ 2.5173 (7)–2.7537 (8) Å], the nonbridged bond length of 2.8264 (8) Å is among the longest yet reported. The existence of an electron pair Fe–Fe bond between Fe(1) and Fe(3) is in accord with the molecule being a closed 48-electron species and the fact that the Fe(1)–Fe(3) separation is substantially shorter than the nonbonded distances of 3.40 Å found in molecules where an Fe–Fe interaction is absent [e.g., $\text{Fe}_2(\text{CO})_6(\mu\text{-PPh}_2)_2^{2-}$, Fe–Fe = 3.630 (3) Å²⁶].

There is a substantial change in the metal framework from 1 to the heavier analogues 2 and 3. Whereas the M_3 triangle is distinctly isosceles in 1, the metal atoms in 2 and 3 define a nearly equilateral triangle with the angles subtended at the metal atoms all close to 60°. Although the longest M–M vector is still associated with the unbridged edge M(1)–M(3) [2, 2.9464 (3) Å; 3, 2.9601 (5) Å], the difference between this distance and the average of the two M(1)–M(2) and M(2)–M(3) bond lengths is considerably less than in the iron compound (1, $\Delta = 0.1635$ Å; 2, $\Delta = 0.0793$ Å; 3, $\Delta = 0.0705$ Å). The Ru–Ru and Os–Os bond lengths in 2 and 3 are within the range of distances observed for related molecules. Some pertinent comparisons are $\text{Ru}_3(\text{CO})_{12}$, 2.8512 (4)–2.8595 (4) Å,²⁷ $(\mu\text{-H})_2\text{Ru}_3(\text{CO})_9(\mu_3\text{-P-tol-p})$ 2.844 (2)–2.937 (2) Å,²⁸ $(\mu\text{-H})_2$

$\text{Ru}_3(\text{CO})_9(\mu\text{-PPh}_2)$, 2.7796 (5)–2.9049 (5) Å,⁹ $\text{Os}_3(\text{CO})_{12}$ 2.877 (3) Å,²⁹ $(\mu\text{-H})\text{Os}_3(\text{CO})_{10}(\mu\text{-PPhH})$, 2.842 (1)–2.888 (1) Å,⁸ $(\mu\text{-H})_2\text{Os}_3(\text{CO})_9(\mu_3\text{-PPh})$, 2.845 (2)–2.972 (3) Å.⁸ The net effect of changing the metal in the series 1–3 thus appears to be a relative strengthening of the unbridged metal–metal bond.

In many, but not all, hydride-bridged clusters the influence of the hydride appears in the form of a lengthening of the bridged metal–metal bond, and this effect has been attributed to closed, three-center, two-electron bonding between the hydrogen atom and the metals. Indeed relative M–M distances, coupled with subtle variations in M–M–CO angles, have been used with success to infer hydrogen atom locations in clusters.³⁰ For 1–3 the M–M bond lengths and solution ¹H and ³¹P NMR spectra might suggest an alternative structure 5, with a double hydride bridge. However, direct location of electron density above and below the M(1)–M(2) and M(2)–M(3) vectors of 1 and 2 and the successful refinement of these hydrogen positions clearly rule out 5. In the present case the presence of a strongly bound $\mu\text{-PPh}_2$ bridge across each of the M(1)–M(2) and M(2)–M(3) edges may be the principal factor responsible for the pattern of M–M bond lengths.



An analysis of the M–P distances (Table III) reveals an asymmetry in the M–P–M bridges with the M(2)–P bond lengths significantly shorter than the M(1)–P and M(3)–P distances which are equivalent [Fe(2)–P = 2.204 (av); Fe(1)–P(2) = 2.257 (1), Fe(3)–P(1) = 2.262 (1), Ru(2)–P = 2.337 (av), Ru(1)–P(2) = 2.393 (1), Ru(3)–P(1) = 2.393 (1), Os(2)–P(2) = 2.345 (av), Os(1)–P(2) = 2.413 (1), Os(3)–P(1) = 2.412 (1) Å]. The M(2)–P bond lengths are closely similar to values found in other clusters where a phosphido group bridges a strong metal–metal bond [e.g., $\text{Fe}_2(\text{CO})_6(\mu\text{-}\eta^2\text{-C}\equiv\text{C-t-Bu})(\text{PPh}_2)$, Fe–P = 2.216 Å (av);¹¹ $\text{Ru}_3(\text{CO})_8(\mu_3\text{-}\eta^2\text{-C}\equiv\text{C-t-Bu})(\mu\text{-PPh}_2)$, Ru–P = 2.341 Å (av);³¹ $(\mu\text{-H})\text{Os}_3(\text{CO})_{10}(\mu\text{-PPhH})$, Os–P = 2.345 Å (av)⁸]. For the ruthenium complex 2 where the X-ray data are of very high precision, asymmetry in the hydride bridges is also evident. Thus the Ru(1)–H(1) [1.64 (5) Å] and Ru(3)–H(2) [1.71 (5) Å] distances are significantly shorter than the $4s$ level than the Ru(2)–H(1) [1.85 (5) Å] and Ru(2)–H(2) [1.92 (4) Å] bond lengths. In total this evidence tends to suggest that there is a stronger association of the

(21) Young, D. A. *Inorg. Chem.* 1981, 20, 2049.

(22) Burt, J. C.; Boese, R.; Schmid, G. *J. Chem. Soc., Dalton Trans* 1978, 1387.

(23) Regragui, R.; Dixneuf, P.; Taylor, N. J.; Carty, A. *J. Organometallics* 1984, 3, 1020.

(24) Cotton, F. A.; Troup, J. M. *J. Am. Chem. Soc.* 1974, 96, 5070.

(25) Andrews, M. A.; Van Buskirk, G.; Knobler, C. B.; Kaesz, H. D. *J. Am. Chem. Soc.* 1979, 101, 7245.

(26) Ginsburg, R. E.; Rothrock, R. K.; Finke, R. G.; Collman, J. P.; Dahl, L. J. *J. Am. Chem. Soc.* 1979, 101, 6550.

(27) Churchill, M. R.; Hollander, F. J.; Hutchinson, J. P. *Inorg. Chem.* 1977, 16, 2655.

(28) Natarajan, K.; Scheidstegger, O.; Huttner, G. *J. Organomet. Chem.* 1981, 221, 301.

(29) Churchill, M. R.; DeBoer, B. G. *Inorg. Chem.* 1977, 16, 878.

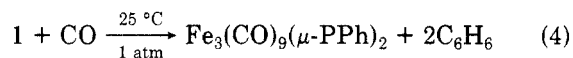
(30) (a) Churchill, M. R.; DeBoer, B. G.; Rotella, F. *Inorg. Chem.* 1976, 15, 1843. (b) Humphries, A. P.; Kaesz, H. D. *Prog. Inorg. Chem.* 1979, 25, 145. (c) Teller, R. G.; Bau, R. *Struct. Bonding* (Berlin) 1981, 44, 1.

(31) Carty, A. J.; MacLaughlin, S. A.; Taylor, N. J. *J. Organomet. Chem.* 1981, 204, C27.

phosphido bridges with M(2) and of the hydrides with M(1) and M(3), emphasizing a contribution to the ground-state description of the molecule in terms of 6.

It is interesting to note that despite an increase in the metal-metal bond lengths of the phosphido-bridged edges in complexes 1-3 on descending the iron triad, the mean M-P-M bond angles (Fe, 73.3°; Ru, 74.6°; Os 74.8°) remain remarkably similar due to a corresponding increase in the M-P bond distances. The acute M-P-M angles are at the lower end of the range of values found for μ -PPh₂ groups and entirely consistent with the presence of a strong M-M interaction.¹¹

Reactivity of $(\mu\text{-H})_2\text{M}_3(\text{CO})_8(\mu\text{-PPh}_2)_2$ toward Carbon Monoxide. As a prelude to a detailed examination of the chemistry of 1-3, we have examined their reactivity toward carbon monoxide. When CO is passed through an *n*-heptane solution of 1 and the solution monitored by IR spectroscopy, the growth of additional $\nu(\text{CO})$ bands can be seen. After 48 h two bands of appreciable intensity at 1966 and 1958 cm⁻¹ are evident. The ³¹P NMR spectrum of this solution exhibits a new resonance at δ +279.4. These spectral features can be attributed to the growth of the phosphinidene complex Fe₃(CO)₉(μ -PPh)₂ (4), the spectral features of which^{17b} were confirmed by an independent synthesis. Integration of the ³¹P NMR resonances indicates a \approx 30% conversion of 1 to 4 after 48 h (eq 4).



Thus intramolecular reductive elimination of benzene from 1 affording the phosphinidene cluster complex 4 is a remarkably ready process. This process in fact becomes rapid at elevated temperatures (60 °C), yielding 4 in essentially quantitative yield within 3 h. Although aryl eliminations from phosphine or phosphido compounds have been described previously,³² such reactions have

usually required rather severe conditions. An increasing number of examples have been described recently where benzene or other hydrocarbon ligand eliminations have occurred under relatively mild conditions,³³ and it has now become clear that such reductive eliminations may be a recurring and complicating factor in the chemistry of low-valent compounds containing phosphine and phosphido ligands.

This marked divergence in reactivity for the heavier congeners of 1 toward CO may be related to the ease of cleavage of the relatively long Fe-Fe bond in 1 (vide supra) by CO to generate an open triangular, 50-electron species 7 with a potentially vacant coordination site on one iron atom. Such an intermediate might "activate" a P-C(phenyl) bond toward reductive elimination in much the same way as that observed for ($\mu\text{-H}$)Ru₃(CO)₉($\mu\text{-PPh}_2$).

Acknowledgment. We are grateful to the Natural Sciences and Engineering Research Council (NSERC) for financial support of this work in the form of grants (to A.J.C.) and scholarships (to A.A.C. and D.N.).

Registry No. 1, 89993-76-0; 2, 87552-32-7; 3, 97689-80-0; 4 (M = Fe), 97689-81-1; [(Ph₃P)₂N]₂[Fe₄(CO)₁₃], 69665-30-1; Ru₃(CO)₁₀(HPPH₂)₂, 97689-82-2; Ru₃(CO)₁₂, 15243-33-1; Os₃(CO)₁₀(Ph₂PH)₂, 97689-83-3; Os₃(CO)₁₀(NCMe)₂, 61817-93-4.

Supplementary Material Available: Tables of anisotropic thermal parameters for non-hydrogen atoms, phenyl ring distances and angles, and structure factors for 1, 2, and 3 (84 pages). Ordering information is given on any current masthead page.

(32) For examples see: (a) Bradford, C. W.; Nyholm, R. S.; Gainsford, G. J.; Guss, J. M.; Ireland, P. R.; Mason, R. *J. Chem. Soc., Chem. Commun.* **1972**, 87. (b) Taylor, N. J.; Chieh, P. C.; Carty, A. J. *J. Chem. Soc., Chem. Commun.* **1975**, 448.

(33) The subject of metal-mediated P-C bond cleavage has recently been reviewed: Garrou, P. *Chem. Rev.*, in press. For references to eliminations from phosphido-bridged ligands see for example ref 1j, 2d, 2g, and: Kikukawa, K.; Matsuda, T. *J. Organomet. Chem.* **1982**, 235, 243.